

**BONE MINERAL DENSITY ESTIMATION USING DIGITAL X-RAY IMAGES FOR
DETECTION OF RHEUMATOID ARTHRITIS****M.VINOTH*¹ AND B.JAYALAKSHMI²**

*¹Post Graduate Student, Department of Computer Science and Engineering,
Sri Venkateswara College of Engineering, Anna University, Chennai, India*
*²Assistant Professor, Department of Computer Science and Engineering,
Sri Venkateswara College of Engineering, Anna University, Chennai, India*

ABSTRACT

Image processing is a widely used domain and its applied in various fields. Biomedical imaging is one of the research areas of image processing which is used to detect diseases. Biomedical imaging consists of various subresearch areas such as bone imaging, cancer imaging, brain imaging and blood cells imaging. The proposed work comes under bone imaging and the objective is to detect the occurrence of Rheumatoid Arthritis (RA). Rheumatoid Arthritis is an autoimmune disease that mainly affects the joints in the human body. Bone organ plays a vital role in identifying these types of diseases. Manual analysis of bone images is a long term process which needs an expert orthopedist for continuous assessment of bone scans which is costly and time consuming. The proposed work involves steps such as denoising, histogram smoothing, segmentation and edge detection in order to enhance the given image and separate the region of interest. The strength of a bone depends on Bone Mineral Density (BMD) which is a major factor in identifying bone diseases and fracture risk. The mathematical relationship between Bone Mineral Content and Volume by Region of Interest will helps in calculating Bone Mineral Density and various features of bone images such as area, mean, standard deviation and variance. The Gray Level Co-occurrence Matrix (GLCM) is one of the image analysis techniques that can be used for extracting features (Energy, Entropy, Contrast, Homogeneity and Correlation) of a bone image. A dataset is created from both the normal and eroded bone images by applying BMD and GLCM features. Whenever a new bone image is given as an input, the features of the image are extracted and compared against the dataset. The input image is classified as whether infected or not infected using neural network which achieved classification accuracy of about 96.66%.

KEYWORDS: Rheumatoid Arthritis, Bone Mineral Density, Gray Level Co-occurrence Matrix and Neural Network.

**M.VINOTH**

Post Graduate Student, Department of Computer Science and Engineering,
Sri Venkateswara College of Engineering, Anna University, Chennai, India

*Corresponding author

1. INTRODUCTION

Visual representation of body parts, organs and tissue is used in diagnosing diseases. In order to create images of body parts for clinical aspects medical imaging is used. Medical imaging provides services for radiologists, radiographers, medical physicists and biomedical engineers to diagnose disease accurately. Medical imaging consists of many advantages: Images are creating an atmosphere for the doctors to diagnose diseases as much as earlier possible. Medical imaging improves the quality of patient results, decrease hospitalization and replace invasive surgeries. Medical imaging produces enormous amount of data and quality of patient care depends on how fast and effectively this data can be turned into high resolution diagnostic images. In real world many people think that Arthritis is a single disease but Arthritis refers to group of more than 100 diseases related to joint stiffness, joint pain and joint inflammation. It not only affects people who are aged but also of all ages, races and genders. Three common and major diseases

under Arthritis are: Osteoarthritis (OA), Rheumatoid Arthritis (RA) and Juvenile Arthritis (JA). Abnormal behavior of cells is a major reason to Rheumatoid Arthritis and its called as chronic that mean long term disease. Some drugs are also used to treat Rheumatoid Arthritis. In this work, we made an attempt to create an automated tool to diagnose Rheumatoid Arthritis as accurate as possible. Basically our immune system should protect our body from foreign cells like bacteria and viruses. Rheumatoid Arthritis is an autoimmune disease which mainly attacks tissue and joints present in the body. Abnormal behavior of immune system causes inflammation that can damage joints and organs. Early morning pain, stiffness, swelling, fatigue and warm, swollen, reddish joints are the symptoms of Rheumatoid Arthritis. Early diagnosis and advanced treatment can control the progress of Rheumatoid Arthritis even though there is no known cure for Rheumatoid Arthritis.

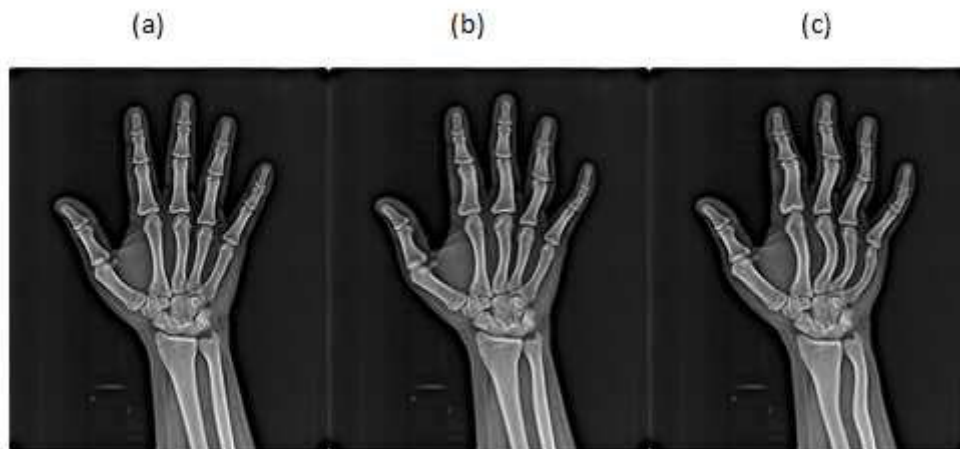


Figure 1

(a) Normal bone image, (b) Partially eroded image, (c) Highly eroded image

Digital image processing plays major role in analysis of images in order to identify these types of diseases. Automated and Efficient tool is needed for analysis of images, extraction of features and classification. The main objective

of this work is to develop automated tool for the diagnosis of Rheumatoid Arthritis that assist radiologist to predict whether the bone is infected or not. The structure of this paper is organized as follows: section 2 describes the

related works of existing system, section 3 describes the System design, section 4 describes results of proposed system, section 5 highlights the conclusion and future work, and then listed the references.

2. RELATED WORKS

In existing system, Bone Mineral Density is measured from images that are obtained from Dual-energy X-ray Absorptiometry (DXA or DEXA), Quantitative Computed Tomography (QCT), Qualitative Ultrasound (QUS), Single Photon Absorptiometry (SPA), Dual Photon Absorptiometry (DPA), Digital X-ray Radiogrammetry (DXR), Single energy X-ray Absorptiometry (SEXA). Craniostenosis, Fibrous dysplasia, Hypophosphatasia, Klippel-Feil syndrome and Osteoarthritis are the diseases that affect bones of a human body and decrease the bone mineral density. This work aims to diagnose Rheumatoid Arthritis which mainly attacks bones of a human body by proposing new procedure or methodology. Many research works are done related to Bone Mineral Density and Gray Level Co-occurrence Matrix. Yeon Soo Lee et al (2012), proposed a method for identifying bone mineral density by reproducible assessment manner that can specify something related to structure reproducible manner. Computed tomography is used to scan back shoulder and front shoulder projection of bone. Then the output images are converted into 3D polygon models. The input format of Mimics v13 software is in STL format. Finite Element model and Mimics v13 software is used to select the region of interest. Rainbow spectrum technique is used to represent the distribution of BMD for various multi material sets. Bone mineral Density was measured based on some mathematical relationship. Repeatability method consist of measurements taken by a single person for the same specimen with intraobserver variance and Reproducibility method consist of measurements taken by two or more people with interobserver [9]. Yoshimichi Hozu et al (2010) proposed a system to analyze Rheumatoid Arthritis and Osteoporosis from CR (Computer Radiography) images. This system uses Discrete Cosine Transform (DCT)

segmentation technique and applies Snakes Algorithm to extract phalanges. Discrete cosine transform is a method of converting image into various formation using mathematical relationships which is used to emphasize the edge of the different images. The bone region is extracted by this operation and each finger is extracted by labelling process. Contour of each finger is extracted using snakes algorithm. Sobel filter is used to obtain the joint line. Morphological operation like Erosion and Dilation are used to extract the features from binary image or gray image. Erosion takes place before dilation while starting the processing. Dilation takes place before erosion while closing the processing. Initial points are placed in neighbourhood of the object in an image. It is used to extract an object by transforming those points based on edge information. From the result we can extract contour of each finger bone successfully. True positive (TP) of 84.6% and False positive (FP) of 11.4% were obtained [11]. Hum Yan Chai et al (2011) proposed a method to automatically analyze the bone X-ray images using GLCM features. Features like Homogeneity, correlation and some other extra features are measured to identify the bone fracture. Femur fractures are taken as sample for analysis. It is classified in to 3 groups namely simple, wedge and complex. K-means algorithm is used to enhance the bone image. Region of Interest (ROI) is identified by segmentation. Sobel and Canny techniques are used to detect the edge of the bone features. Images are grouped as normal femur images and fractured femur images using GLCM based on statistical values like Contrast, Correlation, Energy and Homogeneity. Simulated results show 86.67% of accuracy which leads to efficient method of identifying bone fracture automatically [2]. In this work, we have analyzed the following papers as related works which are Yener N. Yeni et al (2013) [10], Alexander Valentinitsc et al (2012) [1], P. Zerfass et al (2012) [4], S J Gandy et al (2005) [7], X. Zhou et al (2009) [12].

3. SYSTEM DESIGN & IMPLEMENTATION RESULTS

More than 100 digital x-ray bone images are collected from various online databases and hospitals. The main objective of the proposed system is to analyze the Bone Mineral Density (BMD) present at the Region of Interest (ROI)

of bone image. The proposed approach mainly focuses on extracting the features (Gray Level Co-occurrence Matrix) in order to enhance the performance of the automatic diagnosis of Rheumatoid Arthritis. In below, Figure 2 shows that architecture diagram of the proposed system.

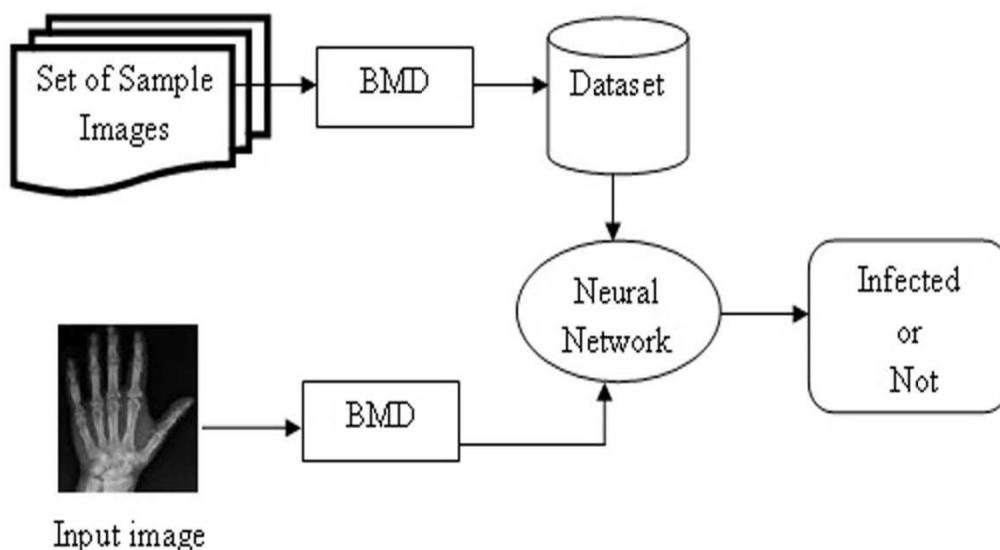


Figure 2
Architecture of Proposed System

Initially set of sample images are taken as input images in order to analyze it in various stages. These sample images contains both normal and eroded images which must be analyzed to create the dataset of the proposed system. This set of sample images are pushed into BMD block one by one. BMD block consist of various steps to be followed such as Denoising using median filter, Smoothing using histogram equalization, Segmentation using Threshold approach, Edge detection using Canny algorithm, Texture feature extraction using Gray Level Co-occurrence Matrix and Calculation of Bone Mineral Density. Figure 3 shows that various steps of BMD block. A

dataset is created based on the BMD and GLCM features of a set of sample images. This dataset is used to train the classifier which gives good accuracy for classification compared to various other classification algorithms. In our proposed system, Neural Network is used for classification. Whenever a new bone image is given as input to the proposed system, it is pushed into the BMD block. Then various steps are performed on this input bone images. Finally BMD and GLCM features are extracted from input bone image. These values are compared against the dataset using neural network and then it is classified as whether infected or not infected.

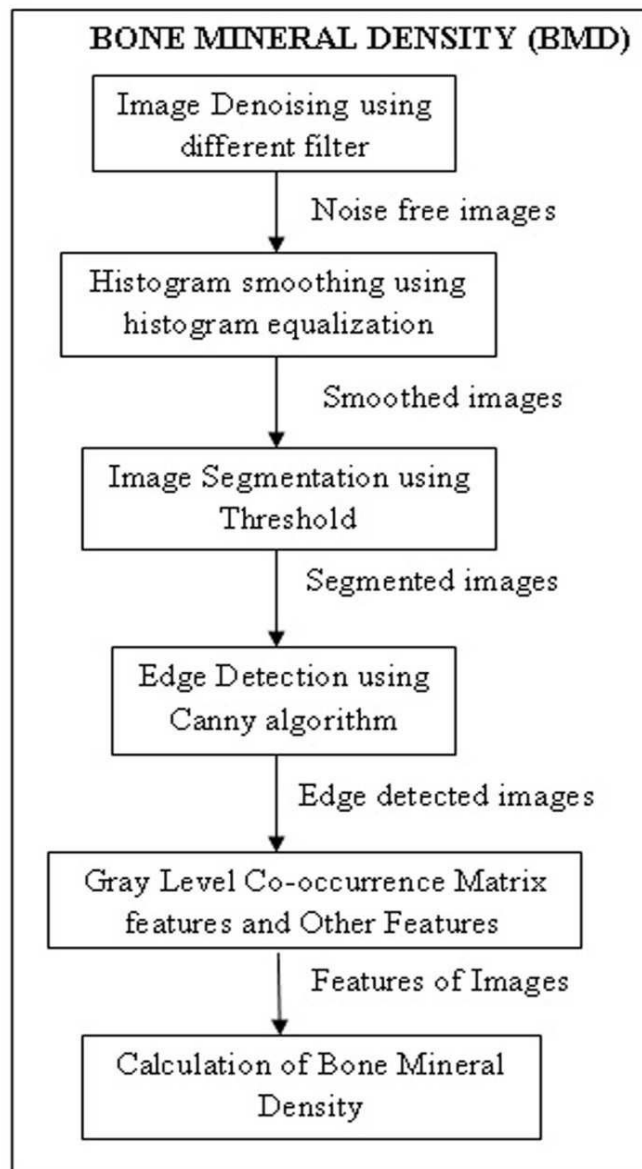


Figure 3
BMD Block Diagram

In this BMD block, there are a list of procedures to be followed such as, enhance the given image, separate the region of interest and extracting features from region of interest. Explanation and important of these procedures are depicted under the following subheadings.

A. Dataset(Image) Collection

Image acquisition is the first and important step in image processing which is used to collect images from various sources such as hospitals, online databases and some other websites. In our proposed system more than

100 digital x-ray images are collected from hospitals. Height, width and resolution of these images are different to one another. In order to produce good accuracy and better performance of proposed system, height, width and resolution of these images are changed as much as possible such that they are similar.

B. Image Preprocessing and Histogram Smoothing

The given input image is converted into gray image. During image acquisition process, image may contain noises but we cannot identify which types of noise are accumulated

in an image. Processing of image without removing noise leads us to get wrong results. So, Image Denoising is most efficient and effective step in image processing. Choosing a filter without knowing which type of noise is present in an image is very difficult and it makes the system to produce inaccurate result. In this work, Some Image quality metrics or

performance parameters are measured in order to choose a filter which gives an average performance on all type of noise [21]. New procedure is created for measuring these performance parameters. From the result of these performance parameters we can identify that median filter gives average performance on all type of noise.

Table 1
Performance parameters for median filter over all type of noise

Parameters/ Noise	MSE	PSNR	NCC	NAE	AD	SC
Salt & Pepper	28.6653	33.5572	0.9866	0.0256	0.3211	1.0208
Poisson	41.0013	32.0028	0.9835	0.0630	0.5138	1.0244
Gaussian	50.9414	26.3427	0.9823	0.1682	0.2483	1.0016
Speckle	56.1443	30.6377	0.9787	0.0770	0.5825	1.0311

Figure 4 shows different types of filters, noise and different type of performance parameters. In preprocessing work, median filter is applied on binary image for removing noise. Smoothing operations are performed using histogram equalization. Histogram smoothing is used to identify the different types of objects appearing in the image and it is very helpful for segmenting region of interest from an image.

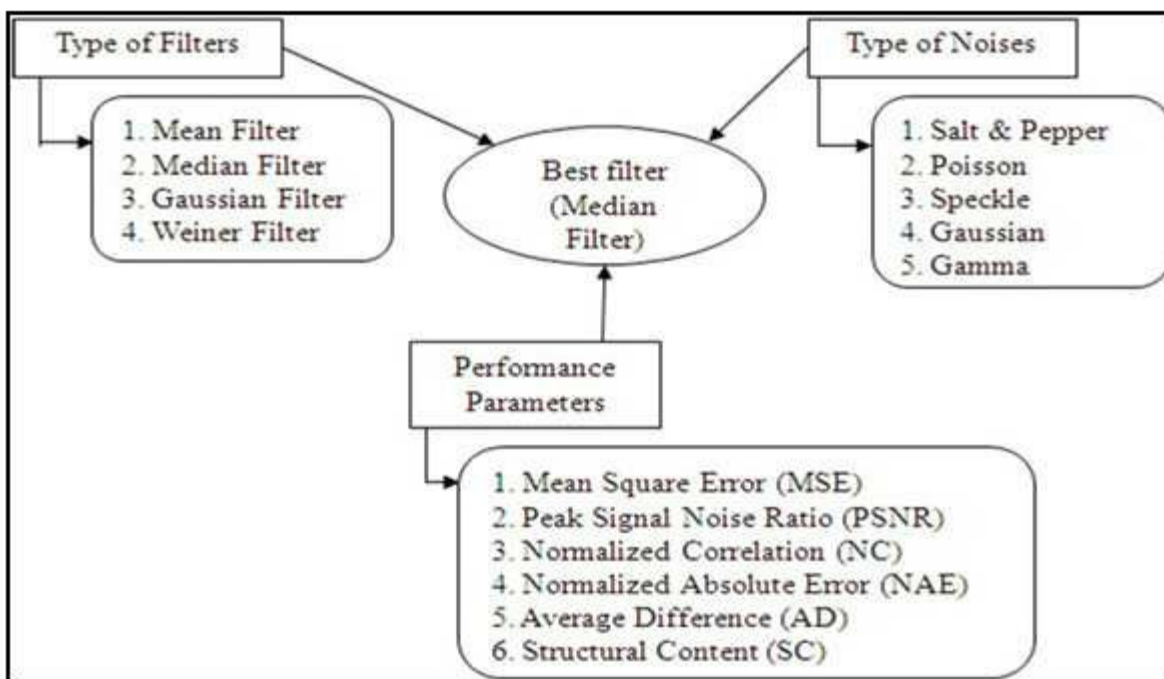


Figure 4
Performance evaluations of various filters

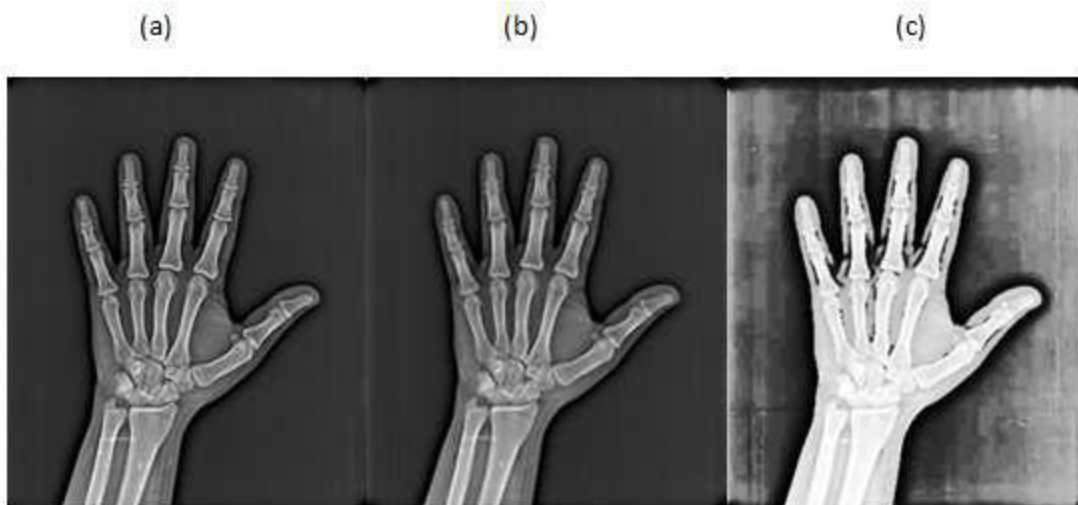


Figure 5

(a) Original Image, (b) Image after applying median filter, (c) Smoothed Image

C. Image Segmentation using Threshold approach

In this work, Segmentation process is done in order to separate the region of interest from an image. In our proposed system, a new approach is proposed to separate the region of interest by drawing ellipse and thresholding. Threshold based segmentation algorithm detects the region of interest more accurately. Edge detection is a very important activity in this work because further process is going to be carried on edge detected image. Canny edge detection algorithm is used to identifying edges of region of interest. In order to identify suitable edge detection algorithm for digital x-ray images, comparative analysis of various edge detection algorithms is done in this work and new procedure is created to calculate time taken by each edge detection algorithm for detecting edges. Speed of edge detection, manual inspection and some parameters such as insensitive to noise and edge localization accuracy are considered to evaluate the performance of various edge detection algorithms. Figure 6 shows various edge detection algorithms, Speed of edge detection and manual analysis for performance evaluation of various edge detection

algorithms. There are some criteria to measure the performance of edge detection algorithms such as speed of edge detection, mathematical measurement, applications and implementation requirements. Basically edge detection algorithms should contain some common functionality:

1. Edge Localization Accuracy (ELA) which refers that location of edge that should be very close as possible to the correct position.
2. Always edges are detected after performing threshold operation in image. Some time high threshold values may lead to false edge detection.
3. Good detection is the major and important characteristic in edge detection. In results, number of false edges should be minimal.
4. Edge detection algorithm can detect edges in image even if it contains noise which refers to noise sensitivity.
5. Efficiency of an algorithm refers to easy implementation and separate processing.
6. Edge detection algorithms should be fast so as to be usable in image processing applications.
7. Post processing is an important activity in edge detection because it is used to reduce noise and suppress non maximum edges.

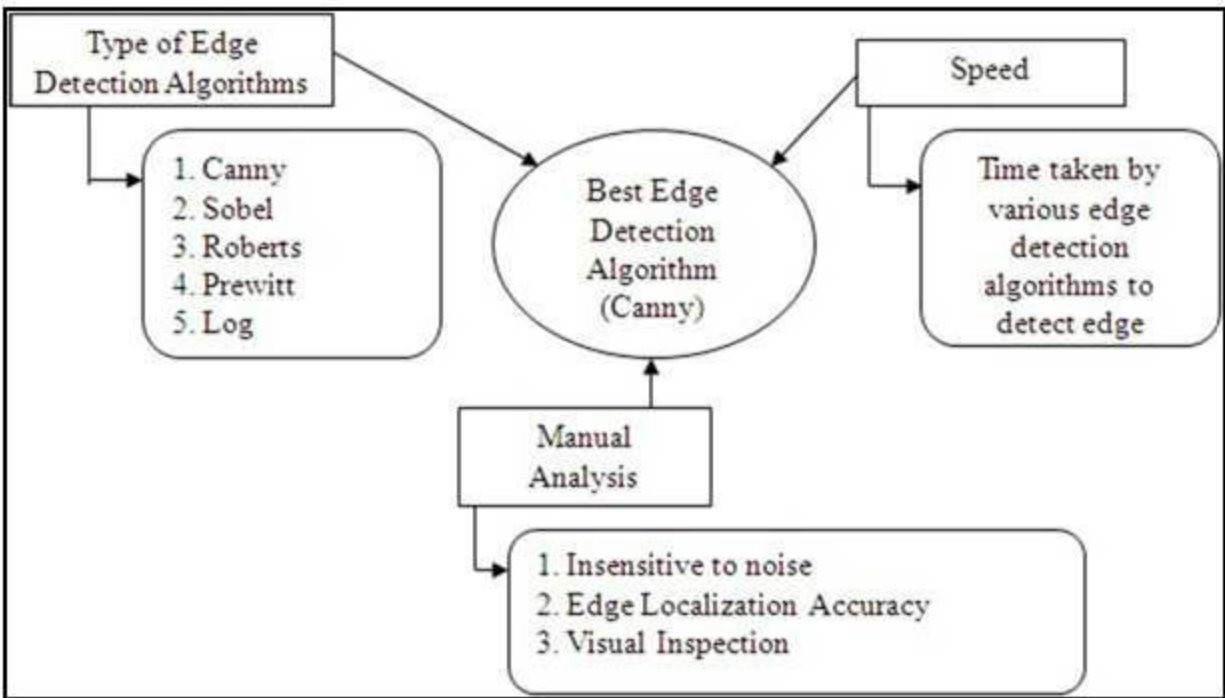


Figure 6
Performance evaluations of various filters

<p>Procedure: Time calculation for various edge detection algorithms to detect edges</p> <pre> tic; tstart1=tic; k=edge(j,'canny'); imshow(k); telapsed1=toc(tstart1); tic; tstart2=tic; l=edge(j,'sobel'); imshow(l); telapsed2=toc(tstart2); tic; tstart3=tic; m=edge(j,'log'); imshow(m); telapsed3=toc(tstart3); tic; tstart4=tic; n=edge(j,'roberts'); imshow(n); telapsed4=toc(tstart4); tic; tstart5=tic; o=edge(j,'prewitt'); imshow(o); telapsed5=toc(tstart5); </pre>	<p>Procedure: Segmentation of region of interest</p> <pre> monochromeImage = k; imshow(monochromeImage); userPrompt = sprintf(' select region of interest'); uiwait(msgbox(userPrompt)); hEllipse = imellipse(gca); xyCoordinates = wait(hEllipse) binaryImage = hEllipse.createMask(); imshow(binaryImage); outputImage = monochromeImage; outputImage(binaryImage) = 255; imshow(outputImage); outputImage = monochromeImage; outputImage(binaryImage) = 0; imshow(outputImage); outputImage = monochromeImage; outputImage(~binaryImage) = 0; imshow(outputImage); </pre>
--	---

In this procedure, time taken by each edge detection algorithm for detecting edges is measured simultaneously. In segmentation procedure, new method is developed in order to select the region of interest by drawing ellipse. Automatic selection of region of interest has a disadvantage that phalanges position in digital x-ray image are differ from one image to another image and joints of phalanges should be take for analysis. In order to produce good accuracy and better performance of proposed system region of interest should be taken

manually. In our proposed system other steps are created in an automatic manner. Initially region of interest is selected by drawing ellipse and then selected portion are segmented. Then the selected portion is mapped with white color and again selected portions are mapped with black color and stored as new image. Finally these white and black images are subtracted in order to identify region of interest. From this, inner portion of region of interest are identified clearly and accurately. Finally edges are detected using canny algorithm from ROI

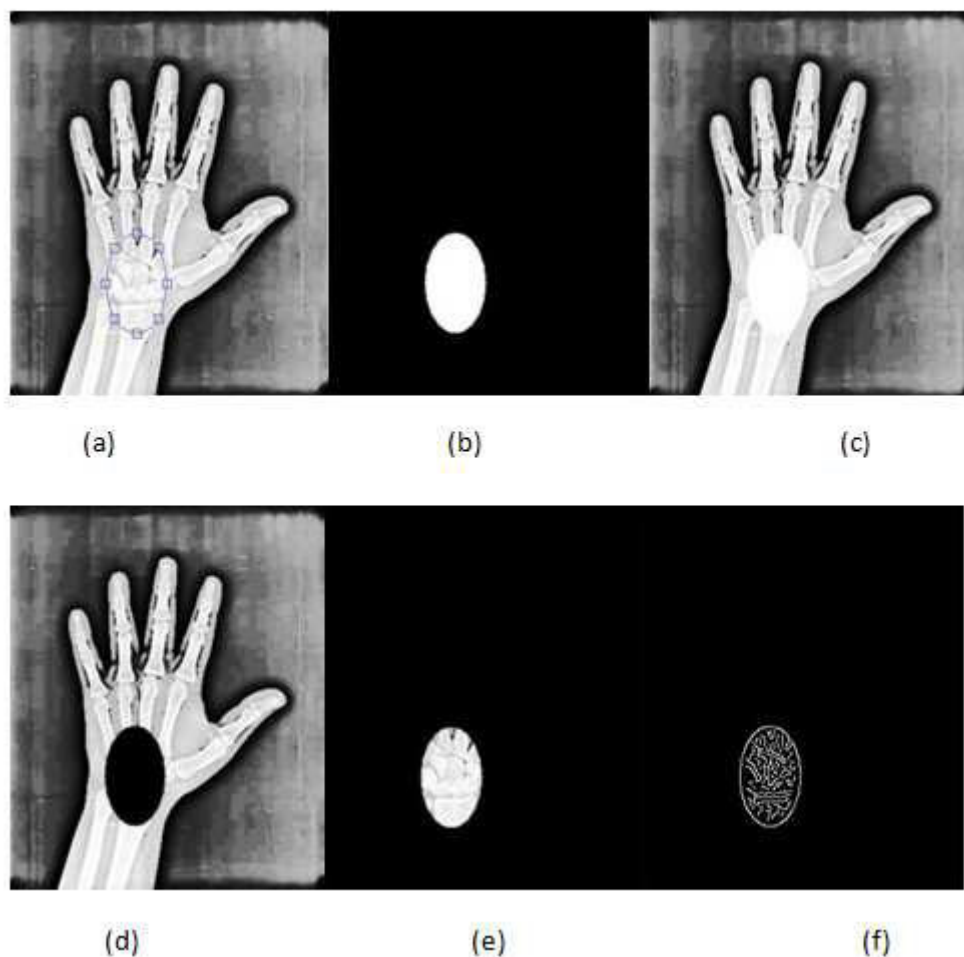


Figure 7
(a) Selection of ROI, (b) Segmented Image, (c) White color mapped Image
(d) Black color mapped Image, (e) Region of Interest, (f) Edge detected Image

D. Bone Mineral Density Calculation and Feature Extraction

In this work, Edge detected image taken as the input and region of interest should be separated from the edge detected image.

Bounding box is one of the image processing novel algorithms which is used to crop the required portion of connected components using maximum and minimum coordinates of edge detected images. Then colors are spread

across cropped image using spread spectrum in order calculate density of region of interest. Bone Mineral Density refers to the amount of mineral present in an area of bone. This work focuses on finding density of bone and do not deal with minerals of bone. We have proposed

a new mathematical relationship and procedure to calculate bone mineral density from the region of interest. Calculation of Bone Mineral Density can be performed using following mathematical relationship.

$$\text{Bone Mineral Density(BMD)} = \frac{\text{Bone Mineral Content (BMC)}}{\text{Volume of Region of Interest (ROI)}}$$

$$\text{Bone Mineral Content (BMC)} = \text{Sum of volume of pixels in ROI} \times \frac{1.073 \text{ grams}}{\text{Calibration of ROI}}$$

$$\text{Volume of ROI} = \pi \left(\frac{\text{diameter}}{2} \right)^2 K$$

Bone Mineral Density is derived from Bone Mineral Content (BMC) of the region of interest and volume of region of interest. BMD is measured in grams/cm³, BMC is measured in grams and volume of ROI is measured in cm³. Sum of volume of pixels in ROI refers to the integrated density of ROI. 1.073 grams is the default value for all the images that refers to the amount of air and water present in bone. Calibration of ROI refers to some measurements of region of interest, in this work perimeter is considered for calculation. Volume of ROI is measured using above mentioned formula. In that formula, diameter is calculated from area of region of interest and k refers to that factor used to identify pixels relationship in an image or length of ROI. In this work, k is calculated using entropy of region of interest/total mean of region of interest. New procedure is created for calculating area, perimeter and integrated density. In this work, Gray Level Co-

occurrence Matrix (GLCM) features (Energy, Entropy, Contrast, Homogeneity and Correlation) for bone images are calculated. GLCM is one of the very famous and popular image analysis techniques which are used to extract above mentioned texture features and classification. GLCM is a statistical way to identify the occurrence of gray level values in an image and to identify how each pixel is related with adjacent pixels. Correlation refers that positively or negatively a pixel is correlated with neighbor pixel. Contrast refers to intensity contrast or brightness of a pixel with its neighbor pixel over whole image. In other way, in a continuous set of pixels, difference between highest and lowest values is contrast. Uniformity of pixels pairs or similarity between pixels is called as energy. Homogeneity returns the values of GLCM to GLCM diagonal by applying closeness distribution of elements. Calculation of GLCM texture features can be performed using below listed formulae.

$$\text{Contrast} = \sum_i \sum_j (i - j)^2 C_{ij}$$

$$\text{Entropy} = \sum_i \sum_j C_{ij} \log C_{ij}$$

$$\text{Energy} = \sum_i \sum_j C_{ij}^2$$

$$\text{Homogeneity} = \sum_i \sum_j \frac{C_{ij}}{1 + |i - j|}$$

In this work, some more features like Mean, Median, Variance and Standard deviation are also derived for both normal and eroded bone images. These values are used for classification because these values will be different for normal and eroded bone images. New procedure is created for calculating Mean, Median, Variance and Standard deviation. Calculation of these features can be performed in this manner. For calculating mean value, intensity value of each pixel are added and

divided by number of pixel in region of interest. For calculating median value, each pixel values are arranged in ascending order. If the count of pixel is odd number, middle value from that ascending order consider as median value. If the count of pixel is even number, then middle two values are taken and average of that two values consider as median value. Variance and standard deviation of region of interest can be calculated from below listed formulae.

$$\text{Mean} = \frac{\text{Sum of pixel values of region of interest}}{\text{Number of pixels in region of interest}}$$

$$\text{Variance } (\sigma^2) = \frac{\sum (X_i - \bar{X})^2}{N}$$

$$\text{Standard Deviation } (\sigma) = \sqrt{\sigma^2}$$

<p>Procedure:</p> <p><i>Area Calculation</i> <code>area=0;</code> <code>[row,col]=size(imcut);</code> <code>for ro=1 : row</code> <code> for co=1:col</code> <code> if(imcut(ro,co) == 0)</code> <code> area=area+1;</code> <code> end</code> <code> end</code> <code>end</code></p> <p><i>Perimeter Claculation</i> <code>perimeter=0;</code> <code>[row,col]=size(imcut);</code> <code>for ro=1 : row</code> <code> for co=1:col</code> <code> if(imcut(ro,co) ~= 0)</code> <code> perimeter=perimeter+1;</code> <code> end</code> <code> end</code> <code>end</code></p> <p><i>Integrated Density Calculation</i> <code>o=rgb2gray(o);</code> <code>[r c]=size(o);</code> <code>s=0;</code> <code>for p=1:c</code> <code> for q=1:r</code> <code> px=impixel(o,c,r);</code> <code> s=px(1,1)+s;</code> <code> end</code> <code>end</code></p>	<p>Procedure:</p> <code>[r,c]=size(A);</code> <p><i>Mean value calculation</i> <code>totmean=sum(A:)/(r*c);</code></p> <p><i>Variance and Standard Deviation</i> <code>totdiff=(A-totmean).^2;</code> <code>totsum=sum(totdiff(:));</code> <code>nele=(r*c)-1;</code> <code>totvar=totsum/nele;</code> <code>totstd=sqrt(totvar);</code></p> <p><i>Median value calculation</i> <code>C=reshape(A,[],1);</code> <code>min1=min(C);</code> <code>max1=max(C);</code> <code>E=sort(A:);</code> <code>num=round((r*c)/2);</code> <code>if (mod(r,2)==0) (mod(c,2)==0)</code> <code> totmedian=(E(num)+E(num+1))/2;</code> <code>else</code> <code> totmedian=E(num);</code> <code>end</code></p>
--	--

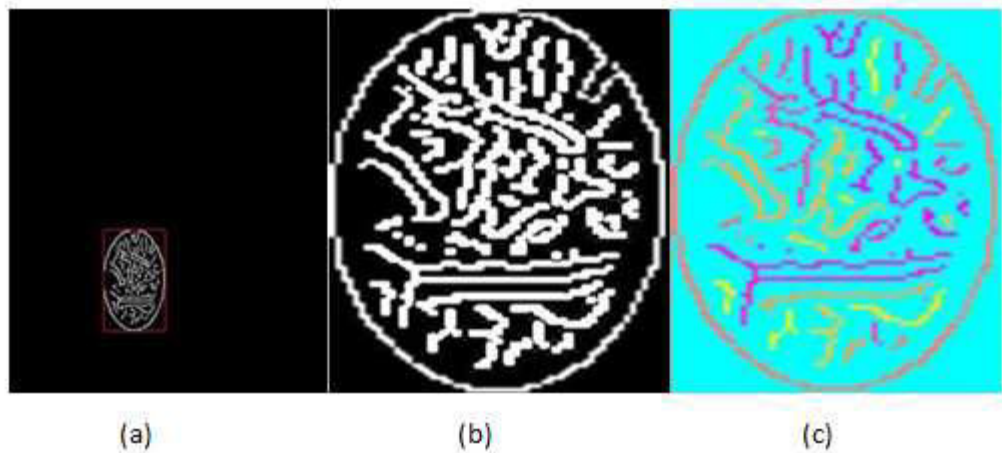


Figure 8

(a) Applying bounding box, (b) Cropped Image, (c) Image after spreading color

E. Analysis of Extracted Features using Neural Network

A dataset is created from both the normal and eroded bone images by applying BMD and GLCM features. Whenever a new bone image is given as an input, the features of the image are extracted and compared against the dataset. The input image is classified as whether infected or not infected using neural network. In this work, neural network is used for classification which gives good accuracy when compared against other classifier. Neural network is organized as layer and perceptron. There are three layers such as input layer, hidden layer and output layer. Input layer is

passive mode and it takes input from outside and simply passed into hidden layer. Hidden layer is active mode and it has many functions such as weighted function which refers to the number of nodes inside the hidden layer and bias function which is used fix the threshold value for network and Sigmoid function which is used active the neural network. Finally output layer is in active mode and it is used to produce the output values as binary. In this proposed system single layer perceptron is taken as classifier which is implemented with hard limit as transfer function and training rule with weighted/bias rule.

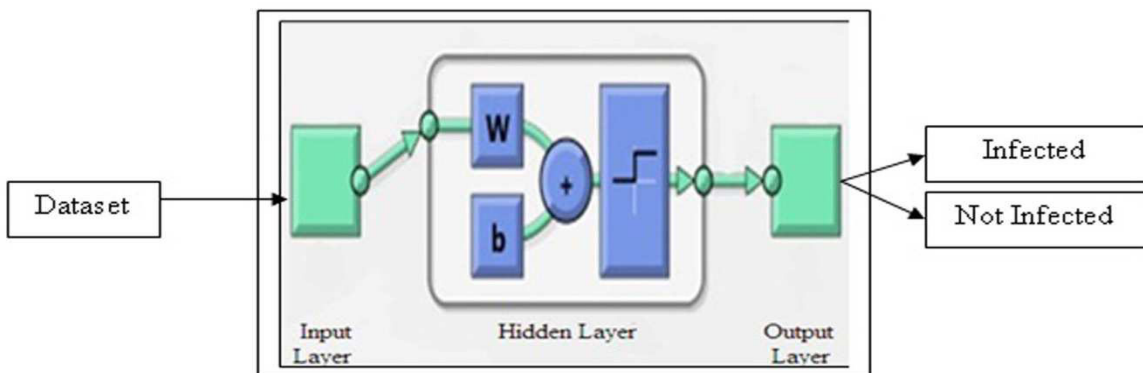


Figure 9

Architecture of neural network

Table 2
Dataset with BMD and GLCM feature for normal and eroded bone images

Image	Area	Perimeter	BMD	Entropy	Mean	Standard Deviation	Contrast	Energy	Correlation	Homogeneity	Integrated Density	RESULT
1	5139	1076	0.8593	0.6648	2.6462	8.0336	11.4614	15.1934	0.7953	0.7287	1192140	Not infected
2	6865	1484	0.7235	0.6751	3.1032	10.4462	12.2634	15.0560	0.7810	0.7311	1187657	Not infected
3	5817	924	0.5732	0.5765	1.3718	5.2531	9.7926	11.6813	0.8251	0.7914	1067998	Infected
4	7003	1061	0.4264	0.5617	1.1491	4.5613	8.9652	11.2151	0.8399	0.7997	1084740	Infected
5	6876	1384	0.8495	0.6521	3.3226	10.3632	11.9060	14.3690	0.7874	0.7434	1167667	Not infected
6	7741	1334	0.5581	0.5923	2.3483	8.2406	10.8925	12.2264	0.8055	0.7817	1087896	Infected
7	7819	1740	0.9443	0.6845	4.7895	13.8908	12.4832	15.4778	0.7771	0.7236	1148889	Not infected
8	5387	1112	0.8056	0.6602	2.5525	7.8554	12.9255	13.7480	0.7692	0.7545	1187568	Not infected
9	7490	1168	0.3715	0.5707	1.1154	3.8749	9.8864	11.3426	0.8235	0.7975	1097766	Infected
10	7002	1134	0.3852	0.5826	1.1404	4.3141	9.8711	11.8381	0.8237	0.7886	1084557	Infected
11	6948	1312	0.5432	0.6315	1.9709	6.7096	11.3448	13.2759	0.7974	0.7629	1090078	Infected
12	4745	1023	0.9542	0.6743	2.8192	8.7038	12.8478	15.3114	0.7706	0.7266	1135689	Not infected
13	6912	1263	0.5463	0.5810	2.5766	8.3195	11.7600	12.8273	0.7900	0.7709	1057899	Infected
14	6298	1318	0.8149	0.6646	3.0737	10.0838	11.7396	15.2087	0.7904	0.7284	1187766	Not infected
15	7052	1162	0.6443	0.6451	1.6626	6.1414	9.8778	11.9434	0.8236	0.7867	1112345	Not infected
16	8383	1418	0.5858	0.5964	2.6581	9.3555	10.8635	12.3538	0.8060	0.7794	1045679	Infected
17	9159	1548	0.5744	0.5961	2.9771	10.4337	10.6172	12.4974	0.8104	0.7768	1078766	Infected
18	7397	1261	0.4677	0.5988	1.5709	5.6394	10.4794	12.3780	0.8129	0.7790	1023458	Infected
19	7174	1183	0.5812	0.5883	2.1188	7.1425	9.5084	12.2515	0.8302	0.7812	1089768	Infected
20	8116	1688	0.9629	0.6627	4.6424	13.2707	11.8896	15.0398	0.7877	0.7314	1197668	Not infected
21	5881	1259	0.9111	0.6720	3.3056	10.2076	11.5380	15.4483	0.7940	0.7241	1135777	Not infected
22	7019	1617	0.9175	0.6957	4.8436	13.4498	12.9418	15.8890	0.7689	0.7163	1167742	Not infected
23	6005	1227	0.7423	0.6569	2.5866	8.1776	12.3052	14.2818	0.7803	0.7450	1141775	Not infected
24	5582	1060	0.5693	0.5873	2.2599	7.1552	10.2740	13.5600	0.8165	0.7579	1090856	Infected
25	6209	1225	0.7531	0.6456	4.6536	14.4726	11.8142	14.1118	0.7890	0.7480	1178765	Not infected
26	6356	1036	0.4351	0.5846	1.1798	4.3242	10.3737	11.2930	0.8148	0.7983	1056752	Infected
27	6174	1284	0.6853	0.6626	2.5131	8.0594	12.5610	14.6079	0.7757	0.7391	1124689	Not infected
28	6456	956	0.3387	0.5546	0.8145	2.8256	9.0781	10.7686	0.8379	0.8077	1034577	Infected
29	5516	1153	0.6624	0.6643	2.1847	7.1324	11.9454	14.8256	0.7867	0.7353	1168998	Not infected
30	6265	1316	0.8732	0.6466	3.0876	10.0838	11.7396	15.2087	0.7904	0.7284	1156789	Not infected

100 bone images are taken as a sample in which 55 is infected images and 45 is not infected images. These images are analyzed by calculating BMD and GLCM features in above mentioned method but in table 2 we have tabulated only for 30 images out of which 14 is infected and 16 is not infected images. This dataset is given into neural network for training. Finally whenever a new bone image is given as an input, the features of the image are extracted and compared against the dataset. The input image is classified as whether infected or not infected using neural network.

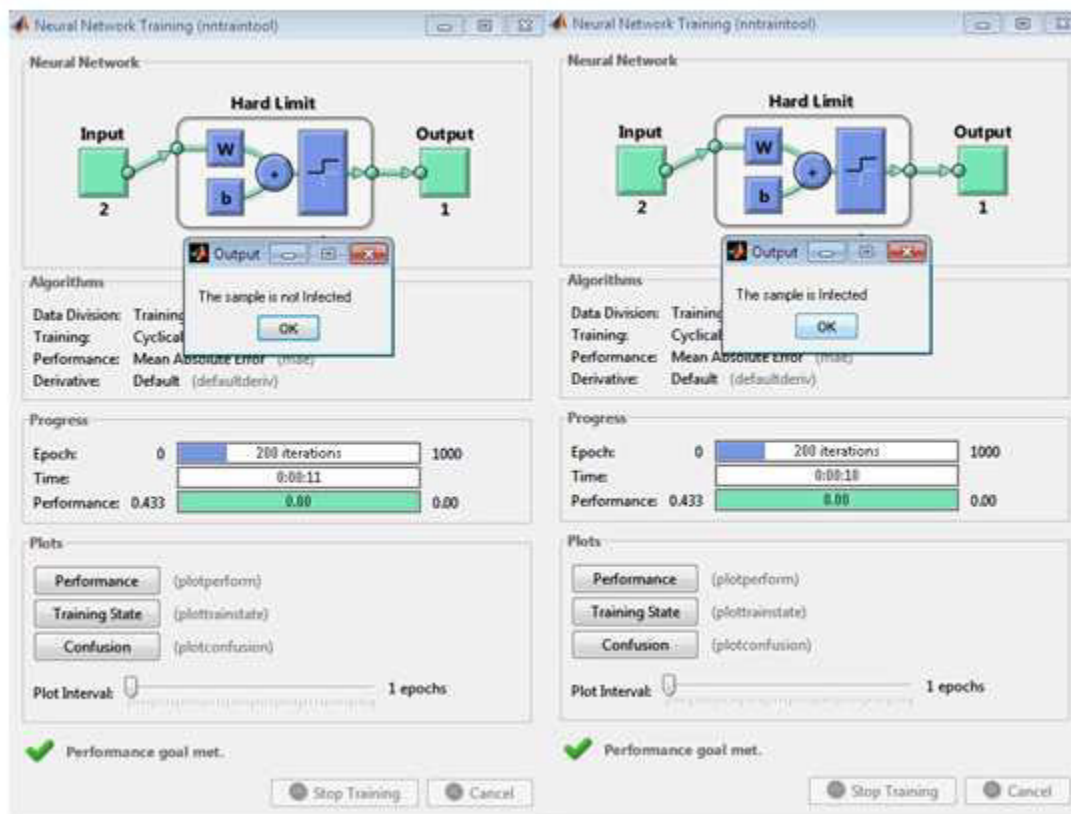


Figure 10
Classification using neural network

F. Performance Evolution

Basically performance of classification can be measured using error rate or accuracy. In this work, performance of proposed system is evaluated in terms of calculating accuracy, precision and recall. These values can be calculated easily by forming confusion matrix

which is also known as contingency table. This confusion matrix contains True Positive (TP), True Negative (TN), False Positive (FP) and False Negative (FN). Recall or sensitivity refers that true positive rate or hit rate and Precision refers positive prediction value and Specificity refers that false positive rate.

$$\text{Accuracy} = \frac{(TP + TN)}{(TP + TN + FP + FN)}$$

$$\text{Sensitivity (Recall)} = \frac{TP}{(TP + FN)}$$

$$\text{Precision} = \frac{TP}{(TP + FP)}$$

$$\text{Specificity} = \frac{TN}{(TN + FP)}$$

Table 3
Confusion matrix of proposed system

Actual		Predicted	
	CONFUSION MATRIX	Infected	Not infected
	Infected	14	1
	Not infected	0	15

Table 4
Performance calculation of proposed system manually

ACCURACY	96.6666
SENSITIVITY	93.3333
SPECIFICITY	100
PRECISION	100

Classifier output

```

=== Run information ===

Scheme:      weka.classifiers.trees.ADTree -B 10 -K -3
Relation:    Dataset Corrected
Instances:   31
Attributes:  12
              Area
              Perimeter
              BMD
              Entropy
              Mean
              Standard
              Contrast
              Energy
              Correlation
              Homogeneity
              Integrated Density
              RESULT
Test mode:   10-fold cross-validation

=== Classifier model (full training set) ===

Alternating decision tree:

: -0.063
| (1)BMD < 0.644: 4.112
| (1)BMD >= 0.644: -4.12
Legend: -ve = Not infected, +ve = Infected
Tree size (total number of nodes): 4
Leaves (number of predictor nodes): 3

Time taken to build model: 0 seconds
                    
```

Classifier output

```

Leaves (number of predictor nodes): 4

Time taken to build model: 0 seconds

=== Stratified cross-validation ===
=== Summary ===

Correctly Classified Instances      28           93.3333 %
Incorrectly Classified Instances     2           6.6667 %
Kappa statistic                     0.8661
Mean absolute error                 0.0845
Root mean squared error             0.2847
Relative absolute error             16.7749 %
Root relative squared error        50.4652 %
Coverage of cases (0.95 level)     93.3333 %
Mean rel. region size (0.95 level) 51.6667 %
Total Number of Instances          30
Ignored Class Unknown Instances     1

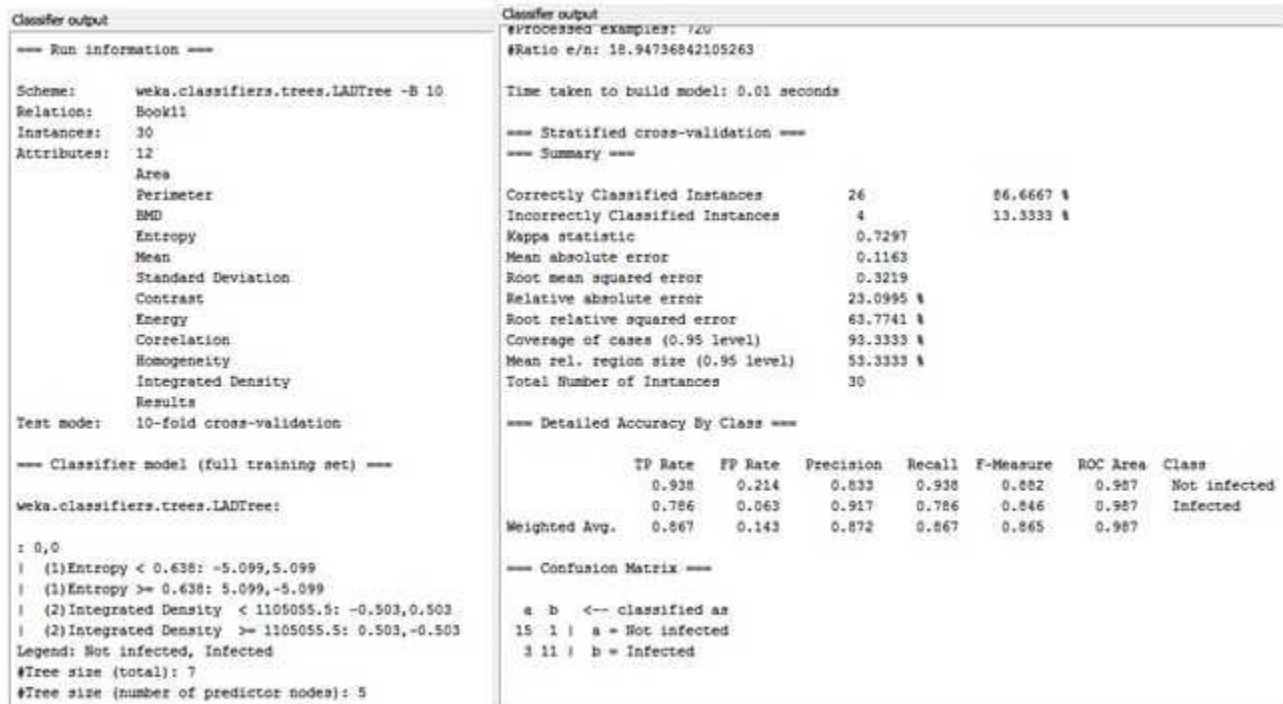
=== Detailed Accuracy By Class ===

                TP Rate  FP Rate  Precision  Recall  F-Measure  ROC Area  Class
                0.938    0.071    0.938     0.938    0.938     0.923    Not infected
                0.929    0.063    0.929     0.929    0.929     0.922    Infected
Weighted Avg.   0.933    0.067    0.933     0.933    0.933     0.923

=== Confusion Matrix ===

 a b  <-- classified as
15 1 | a = Not infected
 1 1 | b = Infected
                    
```

(a)



(b)

Figure 11

(a) Classification by AD Tree, (b) Classification by LAD Tree

Figure 11 shows that automatic classification for dataset (Table 2) using WEKA tool. AD tree classifier gives 0.924 accuracy of classification for proposed system which is less than manually calculated accuracy value. LAD classifier gives that 0.987 accuracy of classification for proposed system which is greater than manually calculated accuracy value. From this we conclude that manually calculated accuracy value using confusion matrix is correct and accurate.

4. CONCLUSION AND FUTURE WORK

Rheumatoid Arthritis is diagnosed using digital x-ray images by applying Gray Level Co-occurrence Matrix (GLCM) features and calculating Bone Mineral Density (BMD). The accuracy of this classifier is evaluated manually as well as automatically using WEKA tool. This classification is more accurate and robust. We can analyze the bone images using this automated tool and we

can predict the status of bone images efficiently. Advantages of the proposed system are quick comparison of images, quantifying changes over time and low cost when comparing to all other existing system. This work can be extended to find the percentage of infection in the bone using fuzzy sets. Rough sets can be used to classify the images that are found unclassifiable.

REFERENCES

- Alexander Valentinitich, Janina M. Patsch, Julia Deutschmann, Claudia Schueller-Weidekamm, Heinrich Resch, Franz Kainberger and Georg Langs (2012), 'Automated threshold-independent cortex segmentation by 3D-texture analysis of

- HR-pQCT scans', Journal of Elsevier bone, Vol. 51, pp. 480–487.
2. Hum Yan Chai, Lai Khin Wee, Tan Tian Swee, Sh-Hussain Salleh, A.K. Ariff and Kamarulafizam (2011), 'Gray-Level Co-occurrence Matrix Bone Fracture Detection', American Journal of Applied Sciences, Vol. 8, No. 1, pp. 26-32.
3. M.N. Bajuria, Mohammed Rafiq Abdul Kadira, Murali Malliga Ramanb and T. Kamarulb (2012), 'Mechanical and functional assessment of the wrist affected by rheumatoid arthritis: A finite element analysis', Journal of Medical Engineering & Physics, Vol. 34, pp. 1294– 1302.
4. P. Zerfass, T. Lowitz, O. Museyko, V. Bousson, L. Laouisset, W. A. Kalender, J.-D. Laredo and K. Engelke (2012), 'An Integrated Segmentation and Analysis Approach for QCT of the Knee to Determine Subchondral Bone Mineral Density and Texture', IEEE Transactions on Biomedical Engineering, Vol. 59, No. 9, pp. 0018-9294.
5. Rafael C. Gonzalez and Richard E. Woods, 'Digital Image Processing', Tom Robbins, Second Edition, 2001.
6. S. Jayaraman, S. Esakkirajan and T. Veerakumar, 'Digital Image Processing', Second Edition.
7. S J Gandy, A D Brett, P A Dieppe, A Maciewicz, C J Taylor, J C Waterton and I Watt (2005), 'Measurement of cartilage volumes in rheumatoid arthritis using MRI', The British Journal of Radiology, Vol. 78, pp. 39–45.
8. Stephen J. Chapman, 'MATLAB Programming for Engineers', Thomson, Third Edition, 2005.
9. Yeon SooLee, TerihisaMihata and JooHanOh, 'Anatomically reproducible assessment of volumetric bone mineral density - Based on clinical computed tomography', Journal of Biomechanics, Vol. 46, pp. 767–772, 2013.
10. Yener N.Yeni, LailaM.Poisson and MichaelJ.Flynn, 'Heterogeneity of bone mineral density and fatigue failure of human vertebrae', Journal of Biomechanics, Vol. 46, pp. 1396–1399.
11. Yoshimichi Hozu, Seiichi Murakami, Hyoungseop Kim, Joo Kooi Tan, Seiji Ishikaw and Takatoshi Aoki (2010), 'Segmentation Method for Phalanges in CR Image by Use of DCT', International Conference on Control, Automation and Systems, Vol. 2, No. 1, pp. 978-89-93215, 2013.
12. X. Zhou, T. Hayashi, H. Chen, T. Hara, R. Yokoyama, M. Kanematsu, H. Hoshi and H. Fujita, 'Automated measurement of bone-mineral-density (BMD) values of vertebral bones based on X-ray torso CT images', 31st Annual International Conference of the IEEE EMBS, Vol. 9, No. 7, pp. 4244-3296, 2009.
13. Samantha J. Polak, Salvatore Candido, Sheeny K. Lan Levengood, Amy J. Wagoner Johnson, "Automated segmentation of micro-CT images of bone formation in calcium phosphate scaffolds", Computerized Medical Imaging and Graphics, Elsevier,2011.
14. Egon Perilli, Andrew M. Briggs, Susan Kantor , John Codrington , John D. Wark , Ian H. Parkinson , Nicola L. Fazzalari , "Failure strength of human vertebrae: Prediction using bone mineral density measured by DXA and bone volume by micro-CT", Bone, Elsevier.
15. Zhu Xiangyang, Yao Lutian, Zhao Lin, Xia Liping, Shen Hui, Lu Jing, "Increased levels of interleukin-33 associated with bone erosion and interstitial lung diseases in patients with rheumatoid arthritis",Cytokine, 2011.
16. Jerome Schmid and Nadia Magnenat-Thalmann, "MRI Bone Segmentation Using Deformable Models and Shape Priors",Springer, Verlag Berlin Heidelberg (MICCAI), pp. 119–126, 2008.
17. E. Lespessailles, C. Gadois, G. Lemineur,J. P. Do-Huu, L. Benhamou, "Bone Texture Analysis on Direct Digital Radiographic Images: Precision Study and Relationship with Bone Mineral Density at the Os Calcis",Springer, 2007.
18. Annamaria Zaia, Roberta Eleonori, Pierluigi Maponi, Roberto Rossi, and Roberto Murri, "Medical Imaging and

- Osteoporosis: Fractal's Lacunarity Analysis of Trabecular Bone in MR Images", IEEE, 2005.
19. Zeinab Nawito, Hanaa M. Rady , Lobna A. Maged. "The impact of fibromyalgia on disease assessment in rheumatoid arthritis patients" Egyptian Society for Joint Diseases and Arthritis, 2013.
 20. Samah A. El Bakry , Iman H. Bassyouni , Reem El-Shazly , Amany A. Abou-El Alla , "Clinical significance of soluble-triggering receptor expressed on myeloid cells-1 in patients with rheumatoid arthritis", The Egyptian Rheumatologist, 2013.
 21. Sp.Cholingam, K.Komathy and M.Sowmya, "Performance Analysis of Various Lymphocytes Images De-Noising Filters over a Microscopic Blood Smear Image", International Journal of Pharma and Bio Sciences, Vol. 4, Issue. 4, 2013.
 22. Subhash Singla MD and Ankur Wadhera, "MRI Imaging Features in Global Hypoxic Ischemia", Intenational Journal of Pharma and Bio Sciences, Vol. 4, Issue. 4, 2013.
 23. Pan Lin, Feng Zhang, Yong Yang, Chong-Xun Zheng, "Carpal-Bone Feature Extraction Analysis in Skeletal Age Assessment Based on Deformable Model"JCS&T Vol. 4 No. 3, 2004.
 24. Prenana B. Yasdhav, M.P. Dabhade and Kashid Girish, "Superbugs: Challenge to Medical Chemistry", International Journal of Pharma and Bio Sciences, Vol. 4, Issue. 4, 2013.
 25. M.Vinoth and B.Jayalakshmi, "Analysis of Edge Detection Algorithms and Denoising Filters on Digital X-Ray Images", The International Journal Of Science & Technoledge, Vol. 2 Issue 2 February,2014.